Impact of the bounds on the direct search for neutralino dark matter on naturalness

Manuel Drees[1,*] and Ghazaal Ghaffari[1,2,†]

[1]Bethe Center for Theoretical Physics and Physikalisches Institut, Universität Bonn, Nussallee 12, D-53115 Bonn, Germany

[2]Sharif University of Technology, Azadi Ave, PO Box: 11365-11155, Tehran, Iran

(Received 14 April 2021; accepted 9 September 2021; published 25 October 2021)

In the minimal supersymmetric extension of the Standard Model (MSSM) the Higgsino mass parameter μ appears both in the masses of the Higgs bosons and in the neutralino mass matrix. Electroweak finetuning therefore prefers small values of $|\mu|$. On the other hand, binolike neutralinos make a good dark matter candidate. We show that current direct search limits then impose a strong lower bound on $|\mu|$, in particular for $\mu > 0$ or if the masses of the heavy Higgs bosons of the MSSM are near their current limit from LHC searches; these bounds on $|\mu|$ are typically much stronger than the ones from collider physics. There is therefore some tension between fine-tuning and neutralino dark matter in the MSSM. We also provide simple analytical expressions which in most cases closely reproduce the numerical results.

DOI: 10.1103/PhysRevD.104.075031

I. INTRODUCTION

Softly broken supersymmetry alleviates the electroweak hierarchy problem [1,2]. In supersymmetric theories there are no quadratically divergent radiative corrections to the masses of Higgs bosons. Increasing lower bounds of the masses of superparticles from searches at the LHC [3] nevertheless imply sizable loop corrections to the masses of Higgs bosons in realistic supersymmetric models. This leads to fine-tuning if soft breaking masses are treated as uncorrelated [4,5]. However, this source of fine-tuning might be greatly reduced in models with a small number of independent soft breaking parameters, typically defined at a very large renormalization scale, which introduce correlations between weak-scale parameters [6].

On the other hand, the minimal supersymmetric extension of the standard model (MSSM) [7,8] also requires a supersymmetric contribution to Higgs and Higgsino masses; this mass parameter is usually called μ. Searches for charginos at LEP imply [3] $|\mu| \gtrsim 100$ GeV. Since μ enters the Higgs potential already at tree-level, a value of $|\mu|$ much above M_Z inevitably leads to fine-tuning. There is thus general agreement in the discussion of fine-tuning issues in the MSSM that—given the experimental lower bound—smaller values of $|\mu|$ are preferred, with the necessary degree of fine-tuning increasing like $|\mu|^2$.

The same parameter μ also sets the mass scale for the Higgsinos in the MSSM[1]; as already noted, this is the origin of the lower bound on $|\mu|$. This establishes a connection between fine-tuning and the phenomenology of the neutralinos and charginos in the MSSM.

One of the attractive features of the MSSM with exact R-parity is that it automatically contains a candidate particle to form the cosmological dark matter whose existence can be inferred from a host of observations, assuming only that Einsteinian (or indeed Newtonian) gravity is applicable at the length scales of (clusters of) galaxies [10]. This candidate is the lightest neutralino $\tilde{\chi}_1^0$ [11], whose mass is bounded from above by $|\mu|$. Given that naturalness arguments prefer a small value of $|\mu|$, one might assume that the most natural dark matter candidate in the MSSM is a light Higgsino-like neutralino. However, in minimal cosmology a Higgsino-like neutralino has the correct relic density only for $|\mu| \simeq 1.2$ TeV [12], which would lead to permille-level electroweak fine-tuning. A winolike LSP would have to be even heavier. One can appeal to nonstandard cosmologies, e.g., including non-thermal production mechanisms, in order to give a lighter Higgsino–light neutralino the correct relic density; however, such scenarios are already quite strongly constrained by indirect dark matter searches [13].

[*]drees@th.physik.uni-bonn.de

[†]ghazalf@uni-bonn.de, ghafari_ghazaal@physics.sharif.edu

[1]This can be avoided only if one introduces additional non-holomorphic soft-breaking Higgsino mass terms [9]; however, most supersymmetry breaking mechanisms do not generate such terms. We will therefore not consider this possibility here.

In this article we therefore assume that the bino mass parameter $M_1 < |\mu|$, so that the LSP eigenstate is dominated by the bino component; M_1 can be taken positive without loss of generality. Also in this case fine-tuning would prefer $|\mu|$ to be not far above M_1. On the other hand, if $|\mu| \simeq M_1$ the LSP has sizable Higgsino and bino components, and hence generically sizable couplings to the neutral Higgs bosons of the MSSM. Such mixed neutralinos tend to have rather large scattering cross sections on matter, in potential conflict with strong lower bounds on this quantity from direct dark matter searches [3]. This is true in particular for the so-called "well-tempered neutralino" [14], a bino-Higgsino mixture with the correct relic density in minimal cosmology.

In this article we explore this connection quantitatively, by deriving a lower bound on the difference $|\mu| - M_1$ from the upper bound on the neutralino-nucleon scattering cross section found by the Xenon collaboration [15]. We do this both numerically, and using a simple approximation for the binolike neutralino eigenstate which is very accurate in the relevant region of parameter space. The resulting lower bound on $|\mu|$ is much stronger than the trivial constraint $|\mu| > M_1$ which follows from the requirement of a binolike LSP; this is true in particular if M_1 and μ have the same sign. An upper bound on $|\mu|$ from fine-tuning considerations therefore leads to a considerably stronger upper bound on M_1 from direct dark matter searches.

A binolike neutralino will often have too large a relic density in minimal cosmology. This can be cured either by assuming nonstandard cosmology (e.g., a period of late entropy production [16,17] or by assuming a low reheat temperature [18]), or—for not too small M_1—by arranging for coannihilation with a charged superparticle, e.g., a $\tilde{\tau}$ slepton [19], which can still have escaped detection by collider experiments if it is close in mass to the lightest neutralino. Neither of these modifications changes the cross section for neutralino-proton scattering significantly. By not imposing any relic density constraint our result thus becomes less model dependent. This, as well as the use of the more recent, and considerably stronger, Xenon-1T constraint and the approximate analytical derivation of the constraint on $|\mu|$, distinguishes our analysis from that of Ref. [20].

The rest of this article is organized as follows. In the following section we review neutralino mixing, both exact and using a simple approximation. We also give the relevant expressions for the neutralino-nucleon scattering cross section, and discuss the accuracy of our analytical approximation. In Sec. III we present the resulting lower bound on the difference $|\mu| - M_1$ as a function of M_1, before concluding in Sec. IV.

II. FORMALISM

In this section we briefly review the neutralino masses and mixings in the MSSM, as well as the spin-independent contribution to neutralino-nucleon scattering.

A. The neutralinos in the MSSM

The neutralinos are mixtures of the two neutral gauginos (the bino $\tilde{B}$ and the neutral wino $\tilde{W}_3$) and two neutral Higgsinos $\tilde{h}_d^0$, $\tilde{h}_u^0$ associated with the two $SU(2)$ Higgs doublets required in the MSSM. The resulting mass matrix in the $\tilde{B}$, $\tilde{W}_3$, $\tilde{h}_d^0$, $\tilde{h}_u^0$ basis is given by [8]:

$$\mathcal{M}_0 = \begin{pmatrix} M_1 & 0 & -M_Z\cos\beta\sin\theta_W & M_Z\sin\beta\sin\theta_W \\ 0 & M_2 & M_Z\cos\beta\cos\theta_W & -M_Z\sin\beta\cos\theta_W \\ -M_Z\cos\beta\sin\theta_W & M_Z\cos\beta\cos\theta_W & 0 & -\mu \\ M_Z\sin\beta\sin\theta_W & -M_Z\sin\beta\cos\theta_W & -\mu & 0 \end{pmatrix}. \quad (1)$$

Here M_1 and M_2 are soft breaking masses for the bino and wino, respectively, μ is the Higgsino mass parameter, θ_W is the weak mixing angle, $M_Z \simeq 91$ GeV is the mass of the Z boson, and $\tan\beta = \langle H_u^0\rangle / \langle H_d^0\rangle$ is the ratio of the vacuum expectation values (VEVs) of the two neutral Higgs fields. The mass matrix is diagonalized by the 4×4 matrix N, such that the ith neutralino eigenstate is given by

$$\tilde{\chi}_i^0 = N_{i1}\tilde{B} + N_{i2}\tilde{W}_3 + N_{i3}\tilde{h}_d^0 + N_{14}\tilde{h}_u^0. \quad (2)$$

Here we are interested in scenarios where the lightest neutralino $\tilde{\chi}_1^0$, which is our dark matter candidate, is dominated by the bino component. This requires $|M_1| < |M_2|, |\mu|$. We will assume that these mass parameters are real; nontrivial complex phases would contribute to CP violation, which is strongly constrained by upper bounds on the electric dipole moments of the electron and neutron [21]. Without loss of generality we take M_1 to be positive, but allow both signs for μ. $|M_2|$ is constrained significantly by searches for charginos and neutralinos at the LHC [3]; as long as $|M_2| \gg M_1$ the sign of M_2 is essentially irrelevant for our analysis.

Evidently the mixing between the gaugino and Higgsino states is controlled by the mass of the Z boson. If the difference between the gaugino masses and $|\mu|$ is larger than M_Z, all mixing angles will therefore be quite small, allowing for an approximate perturbative diagonalization of

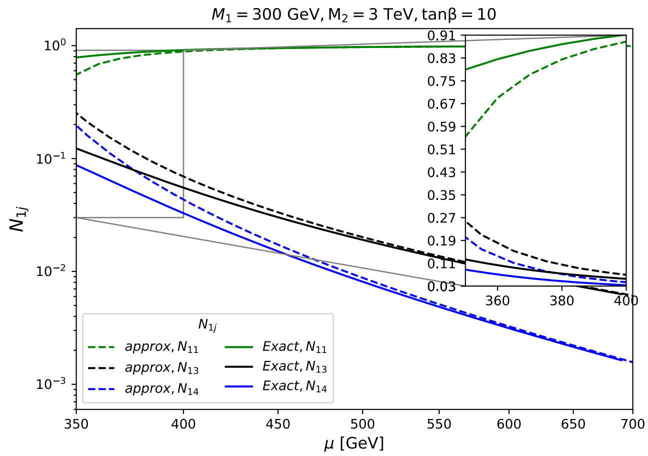

FIG. 1. The bino and Higgsino components of the lightest neutralino eigenstate as a function of μ, for fixed $M_1 = 300$ GeV, $M_2 = 3$ TeV and $\tan\beta = 10$. The simple approximation of eqs. (3) (dashed curves) describes the exact results (solid) very well once $\mu - M_1 \geq 2M_Z$. The insert shows how the two sets of curves approach on a linear scale, for $\mu \leq 400$ GeV.

the mass matrix (1). In particular, the components of a binolike $\tilde{\chi}_1^0$ can then be approximated by [22,23]

$$N_{12} \simeq -M_Z^2 \cos\theta_W \sin\theta_W \frac{M_1 + \mu \sin 2\beta}{(M_1 - M_2)(M_1^2 - \mu^2)};$$
$$N_{13} \simeq -M_Z \sin\theta_W \frac{M_1 \cos\beta + \mu \sin\beta}{(M_1^2 - \mu^2)};$$
$$N_{14} \simeq M_Z \sin\theta_W \frac{M_1 \sin\beta + \mu \cos\beta}{(M_1^2 - \mu^2)};$$
$$N_{11} = \sqrt{1 - N_{12}^2 - N_{13}^2 - N_{14}^2}. \tag{3}$$

In Fig. 1 we compare these approximate expression with exact results. Evidently the approximation works very well for $\mu - M_1 \geq 2M_Z$ or so. Since we took a very large value of M_2 the wino component essentially vanishes in this example; however, the first Eq. (3) shows that it only appears at second order in M_Z, and is therefore always much smaller than the Higgsino components in the region of interest. In this figure we have chosen μ to be positive. The second and third Eq. (3) shows that this increases the Higgsino components. As a result, for $\mu < 0$ the approximation (3) becomes very accurate already for $|\mu| - M_1 \geq 1.5M_Z$.

B. Neutralino-nucleon scattering in the MSSM

In the limit of vanishing neutralino velocity only two kinds of interactions contribute to neutralino-nucleon scattering. One of them depends on the spin of the target nucleus; this contribution is usually subdominant for heavy target nuclei like xenon or germanium, which currently yield the tightest constraints for neutralino masses above 10 GeV or so. The spin independent contributions dominate because their contribution to the scattering cross section off heavy nuclei scales like the square of the nucleon number. They originate from the effective Lagrangian [11]

$$L_{\mathrm{SI}}^{\mathrm{eff}} = f_q \overline{\tilde{\chi}_1^0} \tilde{\chi}_1^0 \bar{q} q \tag{4}$$

which describes the interactions of neutralinos with quarks. Here we have limited ourselves to the leading, dimension-6, operator; strong lower bounds on squark masses [3] imply that dimension-8 operators due to squark exchange [24] can safely be ignored.

Squark exchange also contributes at dimension 6. However, this contribution is proportional to the mass of the quark [11]. That is of course also true for Higgs exchange contributions. However, at least the lighter neutral Higgs boson, whose mass we now know to be 125 GeV, lies about an order of magnitude below the current lower bound on first generation squark masses. For cross sections near the current bound, squark exchange diagrams therefore contribute only at the 1% level at best, which is well below the uncertainty of the Higgs exchange contribution. We therefore ignore them in our analysis.

However, we do allow for the contribution of the heavier neutral Higgs boson. The effective neutralino-quark coupling f_q is thus given by

$$f_q = \sum_{\phi = h,H} m_q \frac{g_{\phi\bar{\chi}\chi} g_{\phi\bar{q}q}}{m_\phi^2}. \tag{5}$$

Note that we factored the quark mass out of the Higgs couplings to quarks, making the latter independent of the quark mass; the couplings to up- and down-type quarks still differ, however. They are given by [25]:

$$g_{h\bar{u}u} = \frac{-g\cos\alpha}{2M_W \sin\beta} \simeq \frac{-g}{2M_W};$$
$$g_{h\bar{d}d} = \frac{g\sin\alpha}{2M_W \cos\beta} \simeq \frac{-g}{2M_W};$$
$$g_{H\bar{u}u} = \frac{-g\sin\alpha}{2M_W \sin\beta} \simeq \frac{g}{2M_W \tan\beta};$$
$$g_{H\bar{d}d} = \frac{-g\cos\alpha}{2M_W \cos\beta} \simeq \frac{-g\tan\beta}{2M_W}. \tag{6}$$

Here α is the mixing angle between the two neutral Higgs bosons, g is the $SU(2)$ gauge coupling and $M_W \simeq 80$ GeV is the mass of the W boson. The couplings of the 125 GeV Higgs boson are known to be quite close to those of the SM Higgs boson [3]. Moreover, none of the heavier Higgs bosons of the MSSM have yet been found. Both observations can easily be satisfied in the so-called decoupling limit, where the mass of the neutral CP-odd Higgs boson satisfies $m_A^2 \gg M_Z^2$. In that limit the other heavy MSSM Higgs bosons also have masses very close to m_A, and the mixing angle α satisfies $\cos\alpha \simeq \sin\beta$, $\sin\alpha \simeq -\cos\beta$. This leads to the simplifications in the Higgs couplings to quarks given after the $\simeq$signs in Eqs. (6). In particular, the couplings of the lighter Higgs boson h then approach those of the SM Higgs, in agreement with observation. The couplings of the heavier neutral Higgs boson H to up-type quarks is suppressed by $1/\tan\beta$, while its couplings to down-type quarks are enhanced by $\tan\beta$. Barring cancellations, H exchange is therefore important only for $\tan^2\beta \gg 1$.

The Higgs bosons couple to one gaugino and one Higgsino current state. As a result, their couplings to neutralino mass eigenstates are proportional to the product of gaugino and Higgsino components [25]:

$$g_{h\tilde{\chi}\tilde{\chi}} = \frac{1}{2} g(N_{12} - \tan\theta_W N_{11})(N_{13}\sin\alpha + N_{14}\cos\alpha);$$
$$g_{H\tilde{\chi}\tilde{\chi}} = \frac{1}{2} g(N_{12} - \tan\theta_W N_{11})(N_{14}\sin\alpha - N_{13}\cos\alpha). \quad (7)$$

Using the approximation (3) and assuming the decoupling limit for the Higgs sector, these become

$$g_{h\tilde{\chi}\tilde{\chi}} = \frac{g' M_Z \sin\theta_W}{2} \frac{M_1 + \mu\sin 2\beta}{M_1^2 - \mu^2};$$
$$g_{H\tilde{\chi}\tilde{\chi}} = \frac{g' M_Z \sin\theta_W}{2} \frac{\mu\cos 2\beta}{M_1^2 - \mu^2}, \quad (8)$$

where $g' = g\tan\theta_W$ is the $U(1)_Y$ gauge coupling.

Equations (8) are the basis for our approximate analytical results. In Fig. 2 we show the ratio of the approximate to the exact $h\tilde{\chi}_1^0\tilde{\chi}_1^0$ coupling as function of $|\mu|$, for $M_1 = 150$ GeV and $\tan\beta = 8$. We see that the approximation works to better than 10% once $|\mu| - M_1 \geq 2M_Z$. For $M_2 = 3$ TeV (which can be taken to represent the limit $M_2 \to \infty$ here)

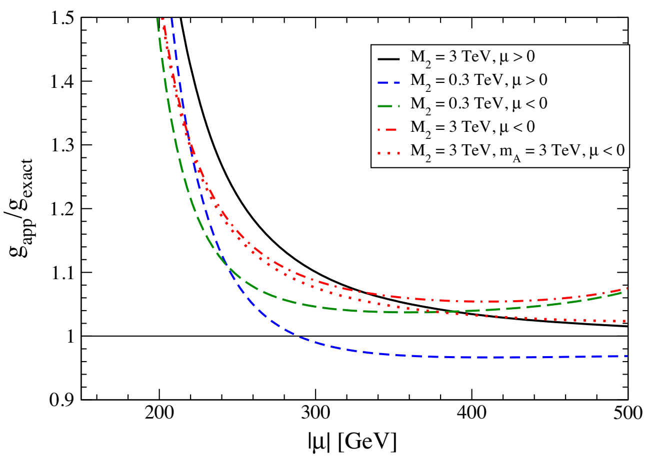

FIG. 2. The ratio of the approximate and exact $h\tilde{\chi}_1^0\tilde{\chi}_1^0$ coupling, given by the first Eq. (7) and the first Eq. (8), respectively, for $M_1 = 150$ GeV and $\tan\beta = 8$. Most curves assume $m_A = 1$ TeV, but the dotted red curve is for $m_A = 3$ TeV.

and large, positive μ (solid black curve) the approximation works to better than 2% even for $m_A = 1$ TeV. Keeping $\mu > 0$ but reducing M_2 to 0.3 TeV, as predicted by gaugino mass unification [8] (short-dashed blue curve) actually improves the quality of the approximation (which assumed $M_2 \to \infty$) for $\mu \lesssim 400$ GeV. The approximation tends to overestimate the true coupling, and allowing a finite M_2 increases the exact coupling, as can be seen from the first Eq. (3): for $M_1 < M_2, |\mu|$, the wino component N_{12} is negative, which increases the absolute value of the first parenthesis in Eqs. (7). Note also that our approximation works to about 5% in this case if μ is large, i.e., the effect of taking $M_2 = 2M_1$ rather than $M_2 \to \infty$ is quite small, as anticipated.

For $M_2 = 3$ TeV and negative μ (dot-dashed red curve) the ratio of approximate and exact results reaches a minimum at $|\mu| \simeq 400$ GeV and then increases again. For some value of μ the $h\tilde{\chi}_1^0\tilde{\chi}_1^0$ coupling vanishes. In our analytical approximation this happens at $\mu = -M_1/\sin(2\beta) = -609$ GeV, as shown by the first Eq. (8), whereas the exact numerical (tree-level) coupling vanishes at $\mu = -602$ GeV. While this differs from the prediction of our approximation only by about 1%, the ratio of the two couplings can deviate from 1 significantly near this zero—in fact, it will diverge at the exact location of the zero. Note also that the red dotted curve, which is for $m_A = 3$ TeV, keeps decreasing even at $|\mu| = 500$ GeV; this indicates that for large $|\mu|$ the main contribution to the (small) deviation between exact and approximate $h\tilde{\chi}_1^0\tilde{\chi}_1^0$ coupling for $m_A = 1$ TeV comes from assuming the decoupling limit in the Higgs sector, rather than from using the approximate neutralino eigenstate (3). Finally, for $m_A = 1$ TeV reducing M_2 to $2M_1$ (long-dashed green curve) again improves the accuracy of the approximation, since it increases the exact coupling, as discussed for $\mu > 0$ above.

One conclusion to be drawn from Fig. 2 is that $M_2 = 2M_1$ and $M_2 \to \infty$ give very similar couplings of the LSP to neutral Higgs bosons, except if this coupling is very small due to a cancellation. Moreover, reducing M_2 in most cases increases the coupling to h, hence the limit of large M_2 gives the weakest, i.e., most conservative, bound on $|\mu|$. We finally note that scenarios with $M_2 = 2M_1$ are quite severely constrained by LHC searches if $M_1 \sim 100$ GeV [26,27]. In the remainder of this article we will therefore assume M_2 to be very large.

The total spin-independent neutralino-proton scattering cross section can be written as [11]

$$\sigma_{\rm SI}^{\chi p} = \frac{4\mu_{\chi p}^2}{\pi} |G_s^p|^2, \quad (9)$$

where $\mu_{\chi p} = m_p m_{\tilde{\chi}_1^0}/(m_p + m_{\tilde{\chi}_1^0})$ is the reduced mass of the neutralino-proton system, and the effective neutralino-proton coupling is given by

$$G_s^p = -\sum_{q=u,d,\ldots} \langle p|m_q\bar{q}q|p\rangle \sum_{\phi=h,H} \frac{g_{\phi\bar{\chi}\chi} g_{\phi\bar{q}q}}{m_\phi^2}. \quad (10)$$

For the light u, d, s quarks, the hadronic matrix elements have to be computed using nonperturbative methods. Once these are known, the contribution from heavy c, b, t quarks can be computed perturbatively through a triangle diagram coupling to two gluons [28]. One usually parameterizes $\langle N|m_q\bar{q}q|N\rangle = f_{T_q} m_p$. We use the numerical values from DarkSUSY [29]:

$$f_{\mathrm{TU}} \equiv \sum_{q=u,c,t} f_{Tq} = 0.14; \quad f_{\mathrm{TD}} \equiv \sum_{q=d,s,b} f_{Tq} = 0.23. \quad (11)$$

We note that these numbers are somewhat uncertain, but our values are rather conservative [30].

Putting everything together, using the approximate expressions (3) for the lightest neutralino eigenstate and assuming the decoupling limit, we find:

$$G_S^p|_h \simeq -A m_p (f_{\mathrm{TU}} + f_{\mathrm{TD}}) \left(\frac{M_1 + \mu \sin 2\beta}{m_h^2(\mu^2 - M_1^2)}\right);$$
$$G_S^p|_H \simeq -A m_p \left(\frac{f_{\mathrm{TU}}}{\tan\beta} - f_{\mathrm{TD}} \tan\beta\right) \times \left(\frac{\mu \cos 2\beta}{m_H^2(\mu^2 - M_1^2)}\right). \quad (12)$$

Here we have introduced the constant

$$A = \frac{g g' M_Z \sin\theta_W}{4 M_W} = 0.032. \quad (13)$$

It should be noted that $\tan\beta > 1$ implies $\cos(2\beta) < 0$. Equations (11) imply that the term $\propto f_{\mathrm{TD}}$ always dominates H exchange. Hence h and H exchange contribute with the same sign if $\mu > 0$ or $\mu \sin 2\beta < -M_1$; they interfere destructively for $0 > \mu > -M_1/\sin 2\beta$.

III. RESULTS

We are now ready to present our numerical results. We wish to determine the lower bound on $|\mu|$ that follows from the nonobservation of neutralinos, which we assume to form all of (galactic) dark matter. We will not be concerned with very light neutralinos, where current bounds from direct dark matter search are still quite poor [3]. For masses above 20 GeV the most stringent current bound comes from the Xenon-1T experiment [15]. In this range the bound is well parametrized by

$$\sigma^{\max}(m_{\tilde{\chi}_1^0})_{\mathrm{XENON}} = \left(\frac{m_{\tilde{\chi}_1^0}}{10\ \mathrm{GeV}} + \frac{2.7\times 10^4\ \mathrm{GeV}^3}{m_{\tilde{\chi}_1^0}^3}\right) \times 10^{-47}\ \mathrm{cm}^2 = \left(\frac{m_{\tilde{\chi}_1^0}}{3.9\ \mathrm{GeV}} + \frac{7\times 10^4\ \mathrm{GeV}^3}{m_{\tilde{\chi}_1^0}^3}\right) \times 10^{-20}\ \mathrm{GeV}^{-2}. \quad (14)$$

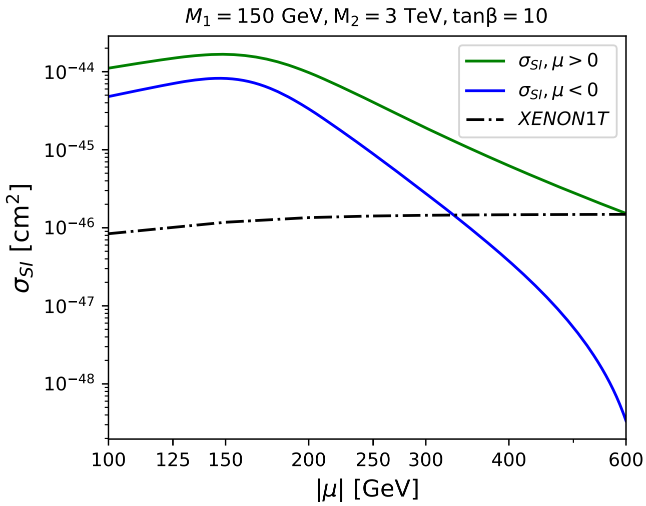

FIG. 3. The predicted neutralino-proton scattering cross section for $M_1 = 150$ GeV, $M_2 = 3$ TeV, $m_A = 1.8$ TeV and $\tan\beta = 10$ as function of $|\mu|$, for positive (green) and negative (blue) μ. The bound from the Xenon-1T collaboration is shown as black dot-dashed line.

Figure 3 shows that this bound constrains the MSSM parameter space quite severely, if we assume that the lightest neutralino $\tilde{\chi}_1^0$ forms all of dark matter. Here we have chosen $M_1 = 150$ GeV, $m_A = 1.8$ TeV, $M_2 = 3$ TeV and $\tan\beta = 10$; we saw at the end of Sec. II that the exact value of M_2 is basically irrelevant as long as it is significantly larger than M_1. As expected the predicted cross section is largest for $|\mu| \simeq M_1$, which leads to strong bino-Higgsino mixing. However, the Xenon-1T bound requires $|\mu|$ well above M_1, i.e., the lightest neutralino has to be binolike; note that values of $|\mu|$ below 100 GeV have not been considered here since they are excluded by chargino searches at LEP for the given (large) value of M_2. We saw above that in the allowed range of $|\mu|$ the approximation (8) works quite well. Equation (12) then explains why the lower bound on $|\mu|$ is considerably weaker for $\mu < 0$: evidently the two terms in the numerator of $G_S^p|_h$ tend to cancel (add up) for positive (negative) μ. As a result, for $\mu < 0$ the contribution from H exchange, which contributes with opposite sign than the dominant h exchange term, is relatively more important and further reduces the cross section. In fact, the h exchange contribution vanishes at $\mu = -M_1/\sin(2\beta) \simeq 760$ GeV. Due to H exchange the actual zero of the cross section [24]—the so-called "blind spot" [31]—already occurs at $\mu \simeq -660$ GeV. In contrast, for $\mu > 0$ the (small) H exchange contribution slightly strengthens the lower bound on μ, which saturates at ~590 GeV for $m_H \to \infty$. This value is already uncomfortably large in view of fine-tuning considerations.

This conclusion is reinforced by Fig. 4, which shows the lower bound on $\mu - M_1$ in units of M_Z as a function of M_1 for four different values of $\tan\beta$; the values of M_2 and m_A

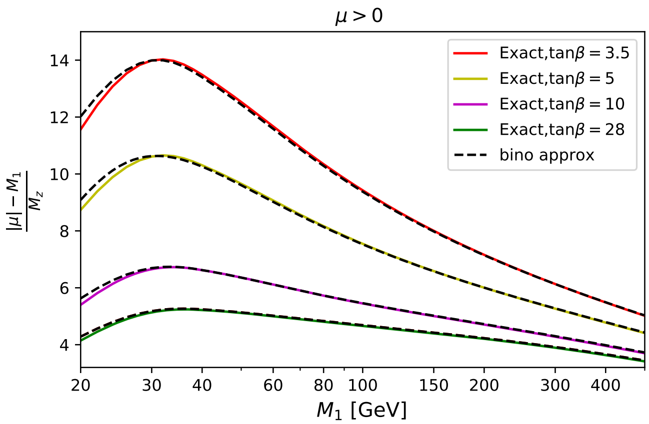

FIG. 4. The lower bound on $|\mu| - M_1$, in units of M_Z, that follows from the upper bound on the neutralino-proton scattering cross section derived by the Xenon-1T collaboration, for $\mu > 0$. We have again chosen $M_2 = 3$ TeV and $m_A = 1.8$ TeV. The solid lines show numerical results obtained using DarkSUSY for different values of $\tan\beta$, while the dashed curves are based on the approximate analytical diagonalization of the neutralino mass matrix, see Eq. (16).

are as in Fig. 3. The solid colored lines have been derived numerically using DarkSUSY, whereas the black dashed lines are based on the approximate diagonalization of the neutralino mass matrix and assume the decoupling limit in the Higgs sector. Recall that we ignore squark exchange, so that only h and H exchange contribute to the spin-independent scattering cross section. Using Eqs. (12) the extremal values of μ that saturate the experimental upper bound on the cross section can be computed analytically. To this end we introduce the quantities

$$\kappa = \frac{\sqrt{\pi\sigma^{\max}}}{2Am_p^2};$$
$$c_\mu = \frac{(f_{\mathrm{TD}} + f_{\mathrm{TU}})\sin 2\beta}{m_h^2} - \frac{(f_{\mathrm{TD}}\tan\beta - f_{\mathrm{TU}}\cot\beta)\cos 2\beta}{m_H^2};$$
$$c_1 = \frac{f_{\mathrm{TD}} + f_{\mathrm{TU}}}{m_h^2}. \tag{15}$$

The quantity A has been defined in Eq. (13), and the normalized hadronic matrix elements f_{TD} and f_{TU} in Eqs. (11). As noted above, the contribution $\propto f_{\mathrm{TU}}$ to the H exchange contribution is essentially negligible. c_μ collects terms in the Higgs exchange amplitude that are proportional to μ; only h exchange contributes to c_1, which gets multiplied with M_1 in this amplitude. The extremal values of μ are then given by

$$\mu_\pm = \frac{c_\mu}{2\kappa} \pm \sqrt{\frac{c_\mu^2}{4\kappa^2} + M_1^2 + \frac{c_1 M_1}{\kappa}}. \tag{16}$$

The dashed lines in Fig. 4 correspond to the positive solution μ_+.

We see that this approximation describes the numerical results very well even for the smallest value of M_1 we consider. In particular, the rather strong dependence on $\tan\beta$ originates from the $\sin 2\beta$ factor in the h exchange contribution to c_μ, see the second Eq. (15); H exchange is always subdominant for our choice $m_H = 1.8$ TeV. The $\tan\beta$ dependence becomes somewhat weaker for larger values of M_1, where the c_1 term becomes more important which is independent of $\tan\beta$.

Evidently the Xenon-1T bound is quite constraining for $\mu > 0$. For example, if we interpret electroweak fine-tuning considerations as requiring $|\mu| < 500$ GeV, one finds $\tan\beta > 10$ for $M_1 \geq 20$ GeV, and $M_1 < 115(165)$ GeV for $\tan\beta = 20(50)$.

We noted above that LHC searches significantly constrain the wino mass parameter if $M_1 \lesssim 100$ GeV; the most sensitive searches are usually those for final states containing three leptons, which dominantly originate from $\tilde{\chi}_1^\pm\tilde{\chi}_2^0$ production. The same searches in principle also probe the production and decay of Higgsino-like states. However, we note that for given mass of the wino- or Higgsino-like states, $\sigma(pp \to \tilde{W}^\pm\tilde{W}^0) \simeq 2\sigma(pp \to \tilde{h}^\pm\tilde{h}^0)$ even after summing over both Higgsino states. Moreover, in the Xenon-allowed region we have $\mu - M_1 > m_h$. The average branching ratio of the two Higgsino-like neutralinos into a Z boson plus LSP is then only about 50%, the other 50% going into h plus LSP, which has much larger backgrounds.[2] LHC constraints on Higgsino-like states are therefore much weaker than those on winolike states; in fact, we are not aware of any published LHC bounds that apply to our scenario, where $M_1 < |\mu| < M_2$.[3] Moreover, we checked that in the Xenon-allowed region, the branching ratios for $h \to \tilde{\chi}_1^0\tilde{\chi}_1^0$ and for $Z \to \tilde{\chi}_1^0\tilde{\chi}_1^0$ are well below the current bounds. In our scenario the strongest bound on μ therefore indeed comes from direct dark matter searches.

As noted in the Introduction, we generally do not require the LSP to have the correct thermal relic density in minimal cosmology. We note that for most of the parameter space shown in Fig. 4 the relic density predicted in this framework comes out much too large if all sfermions are heavy. For example, setting all slepton soft breaking masses to

[2] This can be understood from the electroweak equivalence theorem [32–34] according to which the longitudinal Z boson acts essentially like the neutral would-be Goldstone mode G^0 at sufficiently high energy; in the decoupling limit, G^0 and h reside in the same $SU(2)$ doublet. Exact expressions for the relevant branching ratios can, e.g., be found in Ref. [35].

[3] LHC constraints would also depend on whether or not there are other superparticles with mass between M_1 and μ. For example, for large $\tan\beta$ a single $\tilde{\tau}$ state in this mass range would further reduce the branching ratios of the Higgsino-like states into gauge bosons.

750 GeV, comfortably above recent LHC search limits [36,37], we find $\Omega_{\tilde{\chi}_1^0} h^2$ above 30 (9) for $M_1 = 30(150)$ GeV, and even for LSP mass near $M_Z/2$ the predicted relic density is well above the desired value. An exception occurs for LSP mass near $m_h/2$, where the predicted relic density can even be too low, and comes out just right for two LSP masses slightly above and below $m_h/2$. For $M_1 > m_t$ annihilation into $t\bar{t}$ pairs can reduce the relic density. The size of the corresponding cross section depends on the masses of the $\tilde{t}$ squarks. Their average mass has to be large in order to reproduce $m_h = 125$ GeV, but the mass splitting between the two $\tilde{t}$ states could be large. If both stop masses are above 1.3 TeV, which ensures that all current search limits [38,39] are satisfied, and keeping slepton masses at 750 GeV, we still find $\Omega_{\tilde{\chi}_1^0} h^2 > 3.5$ for $M_1 = 200$ GeV. However, for $M_1 > 100$ GeV the predicted relic density can be made to agree with the measurement even in minimal cosmology by introducing a single light slepton; e.g. for $M_1 = 200$ GeV the correct value is reproduced if there is a right-handed $\tilde{\tau}$ with mass 7 or 8 GeV above the LSP. This would not change the (tree-level) prediction for the LSP scattering cross section.[4] As mentioned in the Inroduction, one can also assume nonstandard cosmology, which (obviously) also would not affect the LSP scattering cross section or LHC phenomenology.

In Eq. (16) we have assumed that $c_\mu \mu + c_1 M_1 > 0$, which is always true for $\mu > 0$. It remains true for values of $|\mu|$ below the "blind spot"; if H exchange is negligible this corresponds to $|\mu| \sin 2\beta < M_1$. The negative solution in Eq. (16) then gives the value of μ where the cross section decreases below the lower bound when coming from $\mu = 0$. Figure 5 shows that this again describes the exact numerically derived bound quite well: although the bound on $|\mu| - M_1$ is considerably weaker than for positive μ, we saw in Eqs. (3) that there are cancellations in the small entries of the $\tilde{\chi}_1^0$ eigenstate if $\mu < 0$; since corrections to this approximation are of order of the squares of these small entries, for given $|\mu|$ the approximation works better for $\mu < 0$. In this figure we only show results for $M_1 \geq 40$ GeV, since for smaller values of M_1 the bound on $|\mu|$ often is below the chargino search limit of about 100 GeV. Note that now the lower bound on $|\mu|$ *in*creases with increasing $\tan\beta$. This is because the "blind spot" $\mu = -M_1/\sin 2\beta$ moves to larger values of $|\mu|$ for larger $\tan\beta$. In the limit $\tan\beta \to \infty$ the bound on $|\mu|$ becomes independent of the sign of μ.

Beyond the blind spot the sign of $c_\mu \mu + c_1 M_1$ flips. This region of parameter space can still be described by Eq. (16),

[4]Since the LSP is a Majorana fermion, $\tilde{\tau} - \tau$ loops can contribute to spin-independent neutralino-nucleon scattering only via Higgs exchange [40], i.e., this would be a quite small correction to the $\tilde{\chi}_1^0 \tilde{\chi}_1^0 (h, H)$ vertices [41].

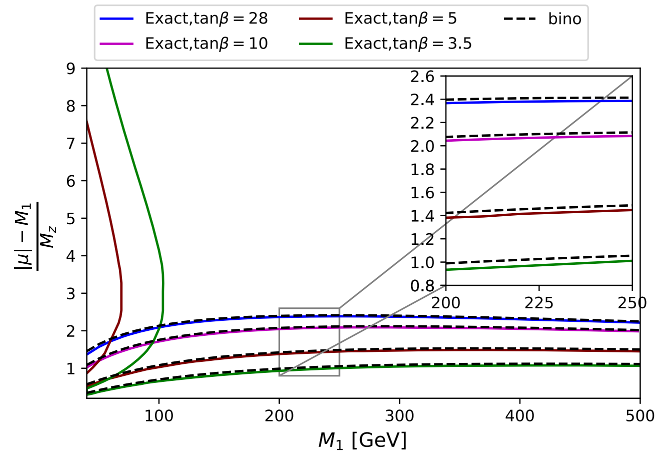

FIG. 5. The lower bound on $|\mu| - M_1$, in units of M_Z, that follows from the upper bound on the neutralino-proton scattering cross section derived by the Xenon-1T collaboration, for $\mu < 0$; the regions to the left of the upper red and green curves are also excluded. Parameter values and notation are as in Fig. 4. The insert shows that our analytical approximation works (even) better for larger values of $|\mu|$, as expected.

by simply setting $\kappa \to -\kappa$ everywhere. If H exchange is negligible, this can easily make the argument of the root in Eq. (16) negative, signaling that no solution exists. In this case the cross section remains below the experimental bound for all values of μ below the μ_- solution in the original eq. (16). For the parameters of Fig. 5 we find that this is true for $\tan\beta > 8$. For smaller values of $\tan\beta$ a sizable region of parameter space (to the left and below the red and green solid lines) beyond the blind spot is again excluded.[5]

So far we have assumed that the heavy Higgs boson is very heavy, so that its contribution to neutralino-proton scattering is subdominant. In fact, there are several constraints on the masses of the heavy Higgs bosons in the MSSM, which can be characterized by the mass of the *CP*-odd Higgs boson, m_A. The most robust bounds come from direct searches for the heavy neutral Higgs bosons; the most sensitive ones exploit their decay into $\tau^+\tau^-$ pairs. In particular, a recent ATLAS analysis [42] is sensitive to m_A up to about 2 TeV, for very large $\tan\beta$. For $\tau^+\tau^-$ invariant masses around 400 GeV there seems to be some excess of events. While not statistically significant, it leads to a bound which is somewhat worse than the expected sensitivity.[6] We therefore chose a parameter set just on the exclusion line, $m_A = 400$ GeV and $\tan\beta = 8$, in order to illustrate the maximal possible effect from heavy Higgs

[5]These curves are reproduced very accurately by the approximate diagonalization of the neutralino mass matrix; we do not show these results in order not to clutter up the figure too much.

[6]CMS did not yet publish the corresponding analysis for the full Run-2 data set.

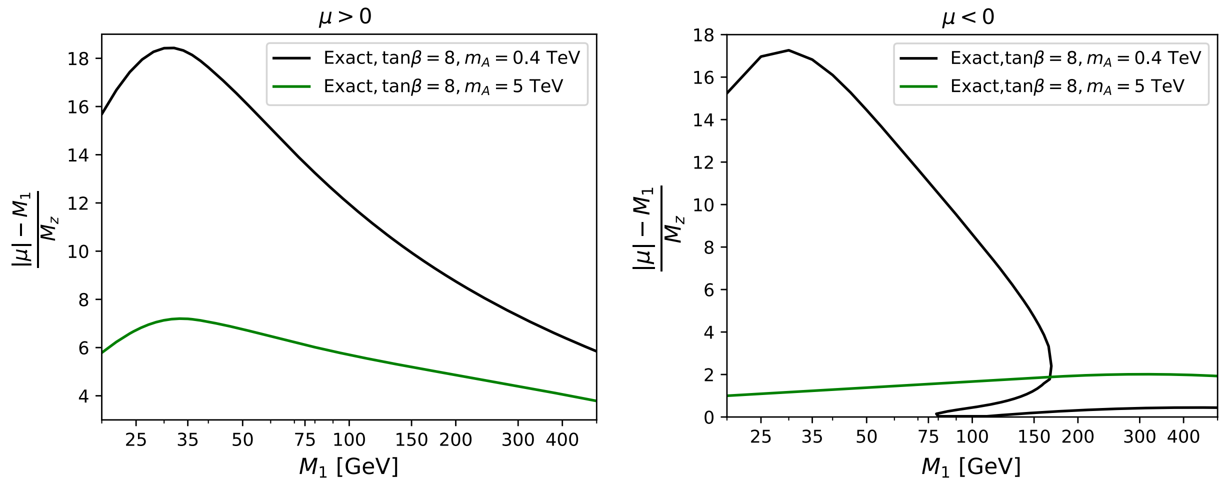

FIG. 6. The lower bound on $|\mu| - M_1$, in units of M_Z, that follows from the upper bound on the neutralino-proton scattering cross section derived by the Xenon-1T collaboration, for $\mu > 0$ (left) and $\mu < 0$ (right). We have chosen $M_2 = 3$ TeV and $\tan\beta = 8$; the black (green) lines are for $m_A = 0.4(5)$ TeV. In the right frame the enclosed region as well as the region below the green or lower black line are excluded.

exchange.[7] It should be noted that this choice leads to a sizable contribution from charged Higgs boson loops to radiative $b \to s\gamma$ decays [43,44]; however, these can be compensated by postulating some amount of squark flavor mixing [45].

The bound on $|\mu|$ that results from the Xenon-1T constraint for this choice of parameters is shown by the black lines in Figs. 6; for comparison we also show results for negligible H exchange (green curves). As noted earlier for $\mu > 0$ both Higgs bosons always contribute with equal sign, so maximizing the H exchange contribution greatly strengthens the lower bound on μ. The effect is especially strong at smaller M_1 since H exchange only contributes to c_μ, not to c_1. The resulting lower bound on μ is always above 950 GeV, i.e., in this region of parameter space a binolike lightest neutralino would yield little benefit regarding electroweak fine-tuning compared with the canonical thermal Higgsino-like neutralino with $\mu \simeq 1.2$ TeV. Of course, the black line shows the *maximal* effect from H exchange. For somewhat larger m_A, away from the ATLAS lower bound, the bound on μ will fall somewhere between the black and green lines.

In sharp contrast, for $\mu < 0$ the H exchange contribution reduces the lower bound on $|\mu|$ even further, by moving the blind spot to smaller values of $|\mu|$. However, for $M_1 \leq 170$ GeV the cross section beyond the blind spot again increases above the Xenon-1T bound, leading to a second excluded region. In fact, the allowed region around the blind spot is very narrow for $M_1 \leq 150$ GeV. The right frame of Fig. 6 therefore shows that for $m_A = 400$ GeV values of M_1 below about 150 GeV require significant fine-tuning, either to hone in on the blind spot, or in the electroweak sector due to the large values of $|\mu|$ required by the Xenon-1T constraint away from the blind spot.

IV. SUMMARY AND CONCLUSIONS

In this paper we have shown that the upper bound on the neutralino-proton cross section from the Xenon-1T experiment leads to strong lower bounds on $|\mu|$ if the bino mass parameter M_1 exceeds 20 GeV. We have assumed that the lightest neutralino forms all of dark matter, but did not require the correct thermal relic density in minimal cosmology. This constraint causes tension with electroweak fine-tuning arguments, since in the MSSM with holomorphic soft breaking terms the Higgsino mass parameter μ also contributes to the masses of the Higgs bosons. The bound is usually significantly stronger for $\mu > 0$; however, also for $\mu < 0$ we found very strong constraints if the heavy Higgs bosons are close in mass to current experimental constraints and $M_1 \leq 150$ GeV. This argument can be turned around to derive an upper bound on M_1 from an upper bound on $|\mu|$ from electroweak fine-tuning; the latter is, however, not easy to quantify unambiguously [46]. In order to give a flavor of possible constraints, let us require the "electroweak fine-tuning parameter" of Ref. [6] to be no larger than 20, (loosely) corresponding to "5% electroweak fine-tuning". This implies $\mu^2 < 10 M_Z^2$, i.e., $|\mu| < 290$ GeV. We see from Fig. 4 that the current Xenon-1T bound is then sufficient to exclude *all* scenarios with $\mu > 0$ and $M_1 \geq 20$ GeV; recall that deviating from the decoupling limit of the Higgs sector (see Fig. 6) or reducing the wino mass (see the discussion of Fig. 2) increases the lower bound on μ even more if $\mu > 0$. The situation for $\mu < 0$ is

[7]We note in passing that this leads to two additional values of M_1 with the correct thermal relic density in minimal cosmology, with LSP mass just above and slightly below 200 GeV; in between these values the predicted relic density will be too low, just as on the h-pole.

more complicated; e.g., for large $\tan\beta$ and large m_A, $|\mu| < 290$ GeV requires $M_1 \leq 100$ GeV (see Fig. 5), but for smaller $\tan\beta$ and/or smaller m_A larger values of M_1 can still be compatible with $|\mu| < 290$ GeV. Our analytical expressions will help to easily update these constraints when future direct dark matter searches are published.

The Xenon-1T bound becomes considerably weaker for neutralino masses below 20 GeV, which we did not consider in this paper. While even very small values of M_1 remain experimentally allowed as long as all sfermions are sufficiently heavy [47], they do not appear particularly plausible given the ever strengthening lower bounds on the masses of the other gauginos (electroweak winos as well as gluinos), chiefly from searches at the LHC [3]. In fact, many models of supersymmetry breaking predict fixed ratios between these masses [48], leading to strong lower bounds on M_1. Our analysis would then lead to even stronger lower bounds on $|\mu|$.

ACKNOWLEDGMENTS

G. G. thanks the Deutsche Akademische Auslandsdienst (DAAD) for partial financial support and the Bethe Center for Theoretical Physics (BCTP) for its hospitality. We thank Hessamaddin Arfaei for discussions.

[1] E. Witten, Nucl. Phys. **B188**, 513 (1981).
[2] N. Sakai, Z. Phys. C **11**, 153 (1981).
[3] P. A. Zyla *et al.* (Particle Data Group), Prog. Theor. Exp. Phys. **2020**, 083C01 (2020).
[4] R. Barbieri and G. F. Giudice, Nucl. Phys. **B306**, 63 (1988).
[5] J. R. Ellis, K. Enqvist, D. V. Nanopoulos, and F. Zwirner, Mod. Phys. Lett. A **1**, 57 (1986).
[6] H. Baer, V. Barger, P. Huang, D. Mickelson, A. Mustafayev, and X. Tata, Phys. Rev. D **87**, 115028 (2013).
[7] H. E. Haber and G. L. Kane, Phys. Rep. **117**, 75 (1985).
[8] H. P. Nilles, Phys. Rep. **110**, 1 (1984).
[9] G. G. Ross, K. Schmidt-Hoberg, and F. Staub, J. High Energy Phys. 03 (2017) 021.
[10] G. Bertone, D. Hooper, and J. Silk, Phys. Rep. **405**, 279 (2005).
[11] G. Jungman, M. Kamionkowski, and K. Griest, Phys. Rep. **267**, 195 (1996).
[12] J. Edsjo and P. Gondolo, Phys. Rev. D **56**, 1879 (1997).
[13] H. Baer, V. Barger, J. S. Gainer, D. Sengupta, H. Serce, and X. Tata, Phys. Rev. D **98**, 075010 (2018).
[14] N. Arkani-Hamed, A. Delgado, and G. F. Giudice, Nucl. Phys. **B741**, 108 (2006).
[15] E. Aprile *et al.* (XENON Collaboration), Phys. Rev. Lett. **121**, 111302 (2018).
[16] M. Kamionkowski and M. S. Turner, Phys. Rev. D **43**, 1774 (1991).
[17] G. B. Gelmini and P. Gondolo, Phys. Rev. D **74**, 023510 (2006).
[18] M. Drees, H. Iminniyaz, and M. Kakizaki, Phys. Rev. D **73**, 123502 (2006).
[19] J. R. Ellis, T. Falk, K. A. Olive, and M. Srednicki, Astropart. Phys. **13**, 181 (2000); **15**, 413(E) (2001).
[20] S. Profumo, T. Stefaniak, and L. Stephenson-Haskins, Phys. Rev. D **96**, 055018 (2017).
[21] A. Arbey, J. Ellis, and F. Mahmoudi, Eur. Phys. J. C **80**, 594 (2020).
[22] M. Drees and M. M. Nojiri, Phys. Rev. D **47**, 376 (1993).
[23] S. Y. Choi, J. Kalinowski, G. A. Moortgat-Pick, and P. M. Zerwas, Eur. Phys. J. C **22**, 563 (2001).
[24] M. Drees and M. M. Nojiri, Phys. Rev. D **48**, 3483 (1993).
[25] J. F. Gunion and H. E. Haber, Nucl. Phys. **B272**, 1 (1986); **B402**, 567(E) (1993) .
[26] A. M. Sirunyan *et al.* (CMS Collaboration), J. High Energy Phys. 03 (2018) 160.
[27] G. Aad *et al.* (ATLAS Collaboration), arXiv:2106.01676.
[28] M. A. Shifman, A. I. Vainshtein, and V. I. Zakharov, Phys. Lett. **78B**, 443 (1978).
[29] T. Bringmann, J. Edsjö, P. Gondolo, P. Ullio, and L. Bergström, J. Cosmol. Astropart. Phys. 07 (2018) 033.
[30] J. Ellis, N. Nagata, and K. A. Olive, Eur. Phys. J. C **78**, 569 (2018).
[31] C. Cheung, L. J. Hall, D. Pinner, and J. T. Ruderman, J. High Energy Phys. 05 (2013) 100.
[32] B. W. Lee, C. Quigg, and H. B. Thacker, Phys. Rev. D **16**, 1519 (1977).
[33] M. S. Chanowitz and M. K. Gaillard, Nucl. Phys. **B261**, 379 (1985).
[34] H. G. J. Veltman, Phys. Rev. D **41**, 2294 (1990).
[35] J. F. Gunion and H. E. Haber, Phys. Rev. D **37**, 2515 (1988).
[36] G. Aad *et al.* (ATLAS Collaboration), Eur. Phys. J. C **80**, 123 (2020).
[37] A. M. Sirunyan *et al.* (CMS Collaboration), J. High Energy Phys. 04 (2021) 123.
[38] G. Aad *et al.* (ATLAS Collaboration), J. High Energy Phys. 04 (2021) 165.
[39] A. M. Sirunyan *et al.* (CMS Collaboration), arXiv:2103.01290.
[40] J. Herrero-Garcia, E. Molinaro, and M. A. Schmidt, Eur. Phys. J. C **78**, 471 (2018).
[41] A. Djouadi, M. Drees, P. Fileviez Perez, and M. Muhlleitner, Phys. Rev. D **65**, 075016 (2002).
[42] G. Aad *et al.* (ATLAS Collaboration), Phys. Rev. Lett. **125**, 051801 (2020).

[43] S. Bertolini, F. Borzumati, A. Masiero, and G. Ridolfi, Nucl. Phys. **B353**, 591 (1991).
[44] F. M. Borzumati, M. Drees, and M. M. Nojiri, Phys. Rev. D **51**, 341 (1995).
[45] K. i. Okumura and L. Roszkowski, J. High Energy Phys. 10 (2003) 024.
[46] M. Drees and S. P. Martin, arXiv:hep-ph/9504324.
[47] H. K. Dreiner, S. Heinemeyer, O. Kittel, U. Langenfeld, A. M. Weber, and G. Weiglein, Eur. Phys. J. C **62**, 547 (2009).
[48] K. Choi and H. P. Nilles, J. High Energy Phys. 04 (2007) 006.